

Vapor–Liquid Equilibrium of Carbon Dioxide–Perfluoroalkane Mixtures: Experimental Data and SAFT Modeling

Ana M. A. Dias,[†] Hervé Carrier,[‡] Jean L. Daridon,[‡] Josep C. Pàmies,^{§,||} Lourdes F. Vega,[§] João A. P. Coutinho,[†] and Isabel M. Marrucho^{*,†}

CICECO, Departamento de Química, Universidade de Aveiro, 3810-193 Aveiro, Portugal, Laboratoire Haute Pression, Centre Universitaire de Recherche Scientifique, Université de Pau, Avenue de l'Université, 64000 Pau, France, and Institut de Ciència de Materials de Barcelona (ICMAB–CSIC), Campus de la UAB, 08193 Bellaterra, Barcelona, Spain

Pressure–composition diagrams were measured at different temperatures ranging from 293.15 to 353.15 K for different perfluoroalkanes including linear (perfluoro-*n*-octane), cyclic (perfluorodecalin and perfluoromethylcyclohexane), and aromatic compounds (perfluorobenzene and perfluorotoluene), at pressures up to 100 bar. Measurements were performed using a high-pressure cell with a sapphire window that allows direct observation of the phase transition. The different molecular structures were chosen in order to check the influence of the nature of the solvent on the carbon dioxide solubility. The soft-statistical associating fluid theory (soft-SAFT) equation of state (EoS) was used to describe the phase behavior of the mixtures studied, searching for transferable parameters with predictive capability. Optimized values for the chain length, Lennard-Jones (LJ) diameter, and dispersive energy are provided for the different perfluoroalkanes and for carbon dioxide. The effect of the explicit inclusion of a quadrupole moment on carbon dioxide, perfluorobenzene, and perfluorotoluene was studied by adding a polar term to the original soft-SAFT EoS.

Introduction

Because of the exceptional solubility of carbon dioxide in perfluoroalkanes, these compounds are being studied for industrial and environmental applications such as the removal of carbon dioxide from gaseous effluents¹ or the improvement of the solubility of hydrophilic substances in supercritical reaction or extraction media.²

In many supercritical fluid applications, carbon dioxide is widely used as the near-critical solvent. As an example, the formation of water in CO₂ microemulsions offers a new approach to biological processes, organic synthesis, nanoparticle chemistry, and dry cleaning³. Although CO₂ has many advantages, its poor solvency with respect to polar compounds can be a problem. Until now, attempts to find suitable hydrocarbon-based surfactants have had a limited success. One strategy that has proven quite successful for overcoming this limitation is to make use of CO₂-philic functional groups to behave as surfactants. It has been verified that the solubility of a compound in carbon dioxide is increased if it contains a fluorinated alkyl segment, since CO₂ is more soluble in fluorinated compounds than in their hydrocarbon counterparts.⁴

Despite this fact, experimental data relating the solubility of CO₂ in perfluoroalkanes is almost inexistent, and to our knowledge, only the mixture CO₂ + *n*-perfluorohexane was studied by Iezzi et al.⁵ at 314.65 and 353.25 K and, more recently, by Lazzaroni et al.⁶ at 313 K. There are two main reasons why more data on this subject are needed: first, perfluoroalkanes are expensive compounds, and so the search

for the best perfluoroalkane to be used in each application becomes an extremely expensive step for the optimal application in a given process; and second, experimental data for different systems and at different conditions can help to elucidate why fluorinated compounds are so soluble in supercritical CO₂ and are far superior surfactants than hydrocarbons, thus promoting the development of more accurate models for these systems.

Several authors employing different techniques and methods have worked on this issue with results leading to different conclusions. To explain the higher solubility of CO₂ in perfluoroalkanes when compared with the corresponding alkanes, some authors suggested a specific solute–solvent interaction between the fluoroalkanes and the CO₂. Cece et al.⁷ justified by ab initio calculations the enhanced binding in the CO₂–C₂F₆ due to the electrostatic interaction between the positively charged carbon atom of CO₂ and the negatively charged fluorine atoms in the perfluoroalkane. Also through ab initio calculations, Raveendran and Wallen² studied the effect of stepwise fluorination on the CO₂-philicity. The authors concluded that CO₂–perfluoroalkane and CO₂–alkane interactions have a different nature, although they are energetically comparable. The perfluoroalkanes interact with CO₂ through its carbon atom, while alkanes interact through the oxygen atoms. These findings agree with the experimental results of Dardin et al.⁸, who, using high-pressure ¹H and ¹⁹F NMR, identified specific solute–solvent interactions, which were qualitatively explained in terms of the surface accessibility of fluorine atoms in the various CF₂CF₃ units in perfluoroalkanes.

Contrary to the previous studies, Diep et al.⁹, using higher levels of theory than those employed in the study by Cece et al.⁷, did not find any particular attraction between CO₂ and perfluoroalkanes, relative to the corresponding alkanes. Furthermore, the authors reported binding energies of CO₂–alkanes ranging from –3.3 to –4.9 kJ/mol, which are slightly higher than those in the CO₂–perfluoroalkanes species. The same conclusions were achieved by Yee et al.¹⁰ through infrared

* Corresponding author. Tel.: +351 234 370360. Fax: +351 234 370084. E-mail: imarrucho@dq.ua.pt.

[†] Universidade de Aveiro.

[‡] Université de Pau.

[§] Institut de Ciència de Materials de Barcelona (ICMAB–CSIC).

^{||} Present address: FOM–Institute for Atomic and Molecular Physics, Kruislaan 407, 1098 SJ Amsterdam, The Netherlands.

spectroscopy, founding no evidence of special attractive interactions between CO₂ and perfluoroethane. Yonker and Palmer¹¹ studied high-pressure ¹H and ¹⁹F NMR spectra of the neat fluorinated methanes and their CO₂ mixtures and concluded that there are no distinct or specific interactions between the fluorinated methanes and CO₂.

Molecular simulations have also been performed for some carbon dioxide/alkane and carbon dioxide/*n*-perfluoroalkane mixtures. Cui et al.¹² carried out a molecular simulation study of the vapor–liquid equilibria of *n*-hexane–CO₂ and perfluoro-*n*-hexane–CO₂ binary mixtures using the Gibbs ensemble Monte Carlo method. The authors did not introduce any binary interaction parameters in their study, and so their results are, in the authors' own words, essentially qualitative. However, the fact that simple interaction-site models correctly predicted the increase of the miscibility for perfluoroalkane–CO₂ compared with the alkane–CO₂ mixture indicates that geometric packing and dispersion interactions have a major role on the miscibility in the two mixtures.

Recently, Gomes and Padua¹³ obtained conformational and structural properties of perfluoroalkanes and alkanes, applying the molecular dynamics method using flexible, all-atom force fields containing electrostatic charges. The authors concluded that it is easier to form a cavity in perfluoroalkanes than in alkanes. This fact can justify the higher solubility of gases in perfluoroalkanes but cannot justify the higher solubility of a bigger molecule, such as CO₂, when compared to other smaller gases, a fact that the authors explain as resulting from differences in solute–solvent interactions. The same study refers that electrostatic terms play a minor role in the interactions between CO₂ and both alkanes and perfluoroalkanes, and that stronger interactions of carbon dioxide with nonpolar solvents should be attributed to dispersion forces and not to any particular affinity of CO₂ for perfluorinated liquids. In a recent work, Zhang and Siepmann¹⁴ presented phase diagrams for selected *n*-alkanes, *n*-perfluoroalkanes, and carbon dioxide ternary mixtures, as a function of pressure, from Monte Carlo simulations. They used two binary interaction parameters for the alkane–perfluoroalkane mixtures, fitted to a particular mixture, and used them in a transferable manner for the rest of the mixtures involving the two compounds. Carbon dioxide was modeled considering the polar charges in an explicit manner, and no binary interaction parameters were used for the carbon dioxide binary mixtures. The agreement with the available data for the binary phase diagrams is fair, and hence, a qualitative agreement with the ternary mixtures is expected. An interesting part of this work is the use of molecular simulations to study the structure and microheterogeneity of the mixtures through the analysis of the radial distribution functions.

Colina et al.¹⁵ studied the phase behavior of mixtures containing carbon dioxide, *n*-alkanes, and *n*-perfluoroalkanes within the context of the statistical associating fluid theory, SAFT, for potentials of variable attractive range (SAFT-VR).¹⁶ In their work, the quadrupole was not treated explicitly but rather in an effective way via the square-well potential of depth ϵ_{11} and adjustable range λ_{11} . They used two binary parameters for the mixtures, fitted to the CO₂/*n*-tridecane mixture. These binary parameters were used to predict the behavior of CO₂/*n*-alkane and CO₂/*n*-perfluoroalkane mixtures, obtaining good agreement for the CO₂/*n*-alkane mixtures but only a fair agreement for the CO₂/perfluorohexane mixture (the only experimental CO₂/perfluoroalkane mixture available). Better results would probably be obtained if the binary parameters were fitted to the

perfluoroalkane mixture specifically. Note also that no electrostatic interactions were explicitly included.

The objective of this work is to check the influence of the molecular structure and the polar interactions on the high-pressure solubility of carbon dioxide in different perfluoroalkanes. New experimental data and modeling results for these systems are presented. The main goal is to contribute with more experimental data relating fluorinated systems and also to get some insight into some of the questions that are still under discussion, such as the role of the quadrupole in these mixtures. For this purpose, a modified version of the statistical associating fluid theory, known as soft-SAFT,^{17,18} was used. This model has already been used to describe experimental data relating the solubility of oxygen and alkanes in perfluoroalkanes,¹⁹ as well as mixtures of carbon dioxide with alkanes and 1-alkanols,²⁰ with high accuracy. In this work, soft-SAFT is used as a tool to infer the role of the quadrupolar interaction for mixtures containing carbon dioxide. For this purpose, a polar term was added to the original soft-SAFT equation of state (EoS) to account for the influence of electrostatic contributions to the global properties of systems containing at least one component with a quadrupole moment. Special care was taken for the physical meaning of the molecular parameters used, as well as the transferability of the binary parameters.

In the next section, the experimental setup and procedure used to measure the solubility of CO₂ in perfluoroalkanes is presented. The modeling section presents the soft-SAFT model, focused mainly in the polar term added to the equation to account for the quadrupole moment on the CO₂ and aromatic molecules. In the results and discussion section, soft-SAFT predictions are compared to the experimental data measured and conclusions are drawn about the influence of electrostatics in the forces ruling these systems.

Experimental Section

Chemicals used for the measurements were perfluoro-*n*-octane (98%) and perfluorobenzene (99%) from Fluorochem, perfluorodecalin (99%) from Flutec, perfluorotoluene (99%) from Apollo Scientific, and perfluoromethylcyclohexane (96%) from ABCR. The carbon dioxide used was from Messer France with a degree of purity >99.9%. Solvents and gas were used with no further purification.

The technique used to carry out vapor–liquid equilibrium measurements with carbon dioxide is based on a synthetic method, which avoids sampling and analyses of both phases. The experimental apparatus used in this work has been described in detail elsewhere, and a good agreement on phase equilibria for the system methane/hexadecane was obtained with literature data.²¹ The experimental apparatus, shown in Figure 1, is essentially made up of a variable-volume high-pressure cell. It consists of a horizontal, hollow stainless-steel cylinder closed at one end by a movable piston. The other end is closed by a sapphire window that allows visual observation of the entire fluid in study. A second sapphire window is fixed on the cylinder wall in order to light the fluid with an optical fiber. This orthogonal positioning of light and observation limits the parasitic reflections and thus improves the observation in comparison to axial lighting. A video acquisition system made up of an endoscope plus a video camera is placed behind the sapphire windows in order to display on the screen of a computer what happens inside the measuring cell. A small magnetic bar is placed inside the cell to allow the homogenization of the mixture by means of an external magnetic stirrer. Because of

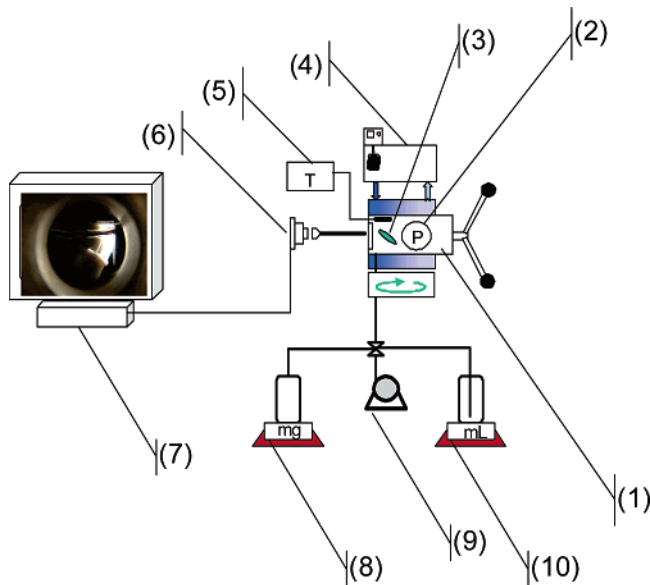


Figure 1. Schematic diagram of the apparatus: (1) high-pressure, variable-volume cell; (2) piezoresistive pressure transducers; (3) magnetic bar; (4) thermostat bath circulator; (5) thermometer connected to a platinum resistance; (6) endoscope plus a video camera; (7) screen; (8) perfluoroalkanes; (9) vacuum pump; and (10) carbon dioxide.

the presence of this magnetic stirring bar as well as of the second window, the minimum internal volume is limited to 8 cm³, whereas the maximum volume was fixed to 30 cm³ to limit the size of the cell and, thus, to reduce thermal inertia and temperature gradients within the cell. The temperature of the cell is kept constant by circulating a heat-carrier fluid through three flow lines directly managed in the cell. This heat-carrier fluid is thermoregulated with temperature stability of 0.01 K by means of a thermostat bath circulator (Haake). The temperature is measured with a high-precision thermometer (AOIP, model PN 5207), with an accuracy of 0.1 K, connected to a calibrated platinum resistance sensor inserted inside the cell close to the sample. The pressure is measured by a piezoresistive silicon pressure transducer (Kulite, model HEM 375, working in the full-scale range of 100 MPa) fixed directly inside the cell to reduce dead volumes. However, as this pressure transducer is placed inside the cell, it is subjected to changes in temperature and it needs to be calibrated. This calibration was done in the temperature range 273–507 K by means of a dead-weight gauge (Bundenberg) with uncertainty better than 0.02%. The uncertainty of the transducer in the experimental range studied is 0.02 MPa.

The binary mixtures are prepared directly in the measuring cell. The cell is first loaded with a known amount of liquid perfluoroalkane by vacuum extraction. The exact mass of liquid introduced is determined by weighing during its introduction in the cell with a precision balance (Ohaus) with an uncertainty of 0.1 mg. The carbon dioxide is then added under pressure. For this purpose, the gas is initially loaded at saturation pressure in an aluminum reservoir tank (Gerzat) loaded on the pan of a high-weight/high-precision balance having a maximum weighing capacity of 2000 g with an accuracy of 1 mg (Sartorius) and connected to the measuring cell by means of a flexible, high-pressure capillary. The needed amount of gas is then transferred from the gas container to the measuring cell. The exact mass of gas injected into the measuring cell is determined by weighing the reservoir tank during filling.

After the mixture of known composition reaches the desired temperature at low pressure, the pressure is slowly increased at

constant temperature until the system becomes homogeneous. During the experiment, the mixture is continuously stirred at high frequency to keep the system in equilibrium during the compression. To avoid supersaturation effects, the fluid phase boundary between the two-phase and the single-phase states is visually observed by measuring the pressure when the second phase is visually observed to disappear. For each temperature, the measure is repeated five times. Reproducibility of the pressure disappearance measurements is within 0.02 MPa.

Soft-SAFT EoS and Molecular Model. SAFT EoSs are generally formulated in terms of the residual molar Helmholtz energy, A^{res} , defined as the molar Helmholtz energy of the fluid relative to that of an ideal gas at the same temperature and density. A^{res} is defined as the sum of several independent microscopic terms whose number depends on the systems under analysis. There are several versions of the SAFT equation available in the literature, most of them differing in the reference fluid.^{16–18,22–24} An excellent review on the development, applications, and different versions of SAFT-type equations was provided by Müller and Gubbins²⁵ and also by Economou.²⁶

The general expression of the soft-SAFT equation used in this work is defined as

$$A^{\text{res}} = A^{\text{total}} - A^{\text{ideal}} = A^{\text{ref}} + A^{\text{chain}} + A^{\text{assoc}} + A^{\text{polar}} \quad (1)$$

A^{ref} accounts for the pairwise intermolecular interactions of the reference system, A^{chain} evaluates the free energy due to the formation of chains from units of the reference system, A^{assoc} takes into account the contribution due to site–site association, and A^{polar} accounts for the electrostatic contribution. The species in this work are nonassociating so that the association contribution to the Helmholtz free energy is zero.

In the soft-SAFT EoS, the reference term is a Lennard-Jones (LJ) monomer fluid, which accounts both for repulsive and attractive interactions. The reference term is calculated using the LJ EoS proposed by Johnson et al.²⁷ When dealing with mixtures, the well-known van der Waals one-fluid mixing rules are used. For the determination of unlike parameters, the generalized Lorentz–Berthelot combining rules are employed,

$$\sigma_{ij} = \eta_{ij} \frac{\sigma_{ii} + \sigma_{jj}}{2} \quad (2)$$

$$\epsilon_{ij} = \xi_{ij} \sqrt{\epsilon_{ii} \epsilon_{jj}} \quad (3)$$

where η and ξ are the binary parameters for the species i and j , which are usually fitted to experimental data. On the basis of the polymerization limit of Wertheim’s theory, A^{chain} is obtained as a function of the chain length of the different species m_i and the pair correlation function of the reference fluid mixture. Hence, the radial distribution function of LJ monomers g_{LJ} is used in the soft-SAFT EoS.

$$A^{\text{chain}} = N_m k_B T \sum_i x_i (1 - m_i) \ln g_{\text{LJ}} \quad (4)$$

where N_m is the number of molecules in the system, with $\rho_m^i = N_m^i/V$ being the molecular density; k_B is the Boltzmann constant; T is the temperature; x_i is the mole fraction of component i ; and the summation extends for all i compounds in the mixture.

The leading multipole term for fluids of linear symmetrical molecules, like carbon dioxide, nitrogen, acetylene, etc., is the quadrupole–quadrupole potential.²⁸ An expansion of the Helmholtz free energy in terms of the perturbed quadrupole–

Table 1. Soft-SAFT Molecular Parameters for CO₂ and Perfluoroalkanes^a

component	m	σ (nm)	ϵ/k_B (K)	Q (C·m ²)	ref	AAD (%) Pvap	AAD (%) density
CO ₂	2.681	253.4	153.4		36	0.25	0.44
CO ₂	1.571	318.4	160.2	4.4×10^{-40}	36	0.50	0.90
C ₆ F ₆	3.148	364.7	253.6		37	3.61	0.19
C ₆ F ₆	3.253	360.2	245.5	5.0×10^{-40}	37	2.39	0.30
C ₇ F ₈	3.538	376.4	253.0		37	3.11	0.52
C ₇ F ₈	3.636	372.3	246.5	5.0×10^{-40}	37	2.63	0.40
C ₈ F ₁₈	3.522	452.1	244.7		19	3.66	0.09
C ₇ F ₁₄	3.463	415.0	228.6		38	0.16	1.73
C ₁₀ F ₁₈	2.696	499.9	310.1		37	3.80	0.05

^a Also presented are the references for the experimental data used to adjust the molecular parameters and the absolute average deviations between experimental data and the correlation given by the soft-SAFT EoS.

quadrupole potential with the Padé approximation was proposed by Stell et al.:²⁹

$$A^{qq} = A_2^{qq} \left(\frac{1}{1 - \frac{A_3^{qq}}{A_2^{qq}}} \right) \quad (5)$$

Expressions for A_2 and A_3 , the second- and third-order perturbation terms, were derived for an arbitrary intermolecular reference potential^{30,31} and involve the state variables, molecular parameters, and the integral J for the reference fluid. A detailed derivation of these expressions is given elsewhere.²⁸ This new term in the soft-SAFT EoS involves an additional molecular parameter, Q , the quadrupolar moment.

Within the soft-SAFT context, perfluoroalkanes and carbon dioxide are modeled as fully flexible LJ chains of length m . The molecular parameters for the perfluoroalkane molecules are then as follows: m , the chain length; σ , the size parameter; and ϵ , the energy parameter. These parameters were obtained by fitting the experimental vapor-pressure and liquid-density data following the procedure described in our previous work.¹⁹

When the quadrupole moment is explicitly taken into account, two more parameters have to be considered, the quadrupolar moment Q and x_p , defined as the fraction of segments in the chain that contain the quadrupole.³² In this work, it was considered that carbon dioxide, perfluorobenzene, and perfluorotoluene present a quadrupole moment.

Experimental values for the quadrupole moment in carbon dioxide and perfluorobenzene are available in the literature.^{33,34} No reference was found regarding the quadrupole in perfluorotoluene, but knowing that the quadrupole moment for benzene is similar to that of toluene³⁵ and that of perfluorobenzene although with a opposite sign,³⁴ it is legitimate to assume that the quadrupole in perfluorotoluene will be similar to that in perfluorobenzene and with the same sign. Regarding the molecular parameter x_p , it was fixed to $1/3$ for carbon dioxide and $1/6$ for perfluorobenzene and perfluorotoluene, mimicking the molecules as three and six segments with a quadrupole in one of them. Therefore, with x_p and Q fixed, only the usual m , σ , and ϵ parameters need to be adjusted. They were readjusted in the usual way by fitting vapor pressure and saturated-liquid densities to experimental data. The values for the quadrupole moments Q for these molecules obtained from the fitting are in agreement with the ones present in the literature.^{33,34} The parameters for all the components studied in this work are presented in Table 1. References for the experimental vapor-pressure and density data used to adjust the molecular parameters and the quadrupole moment are indicated in the table together with the absolute average deviation (AAD) between experi-

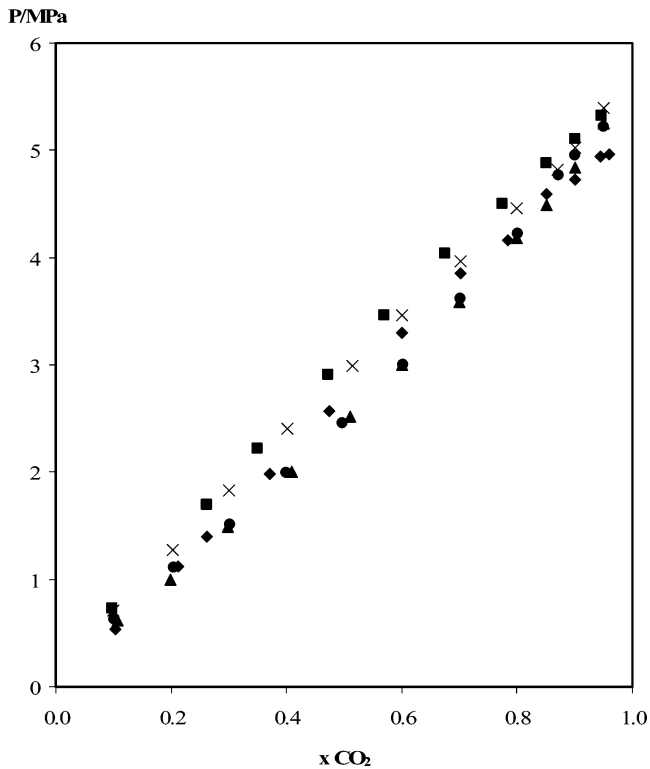


Figure 2. Experimental measured solubility of CO₂ in perfluoroalkanes at 293.15 K: perfluoro-*n*-octane (◆), perfluorodecalin (■), perfluorobenzene (▲), perfluorotoluene (⊗), and perfluoromethylcyclohexane (⊗).

mental data and the predictions given by the soft-SAFT EoS. Vapor pressures and liquid densities are fitted to experimental data with an AAD less than 3.8% and 1.7%, respectively.

Results and Discussion

High-pressure phase diagrams for the mixtures CO₂/perfluoro-*n*-octane, CO₂/perfluorodecalin, CO₂/perfluorobenzene, CO₂/perfluorotoluene, and CO₂/perfluoromethylcyclohexane, at temperatures ranging from 293.15 to 353.15 K, were measured. Experimental results obtained for the five mixtures studied are reported in Table 2.

Figures 2 and 3 compare experimental data at the lowest and highest temperatures measured, respectively. It can be observed that the solubility of the CO₂ in different compounds is very similar, with the differences being larger near the critical point of CO₂. However, some differences should be noted: the solubility of CO₂ in perfluorodecalin is always smaller than in the linear perfluoroalkane (perfluoro-*n*-octane). The solubility of CO₂ in perfluoromethylcyclohexane is between that in perfluorodecalin and that in perfluoro-*n*-octane. At lower temperatures, the aromatic compounds present the highest CO₂ solubility and no significant difference can be observed between them. The temperature effect on the solubility is more pronounced for the aromatic perfluoroalkanes than for the saturated compounds. To address a possible chain size effect on the solubility of CO₂, data measured in this work for perfluoro-*n*-octane were compared with data measured by Iezzi et al.⁵ for perfluoro-*n*-hexane at 314.65 and 353.25 K. As shown in Figure 4, also in this case, no significant difference was found between the two systems except near the critical point at higher temperatures, where the CO₂/perfluoro-*n*-octane presents a slightly more extended two-phase region.

The effect of fluorination was also checked by comparison, whenever possible, between CO₂/perfluoroalkane mixtures

Table 2. P (MPa)– x_{CO_2} – T (K) Data for CO_2 –Perfluoroalkane Mixtures at Different Temperatures from 293.15 to 353.15 K

x_{CO_2}	293.15 K	303.15 K	313.15 K	323.15 K	333.15 K	343.15 K	353.15 K
CO_2 –perfluoro- <i>n</i> -octane (C_8F_{18})							
0.104	0.53	0.59	0.65	0.71	0.78	0.84	0.90
0.212	1.12	1.25	1.38	1.51	1.63	1.76	1.89
0.261	1.39	1.57	1.74	1.91	2.09	2.26	2.44
0.370	1.98	2.26	2.53	2.80	3.07	3.35	3.62
0.473	2.57	2.94	3.32	3.70	4.08	4.46	4.84
0.601	3.29	3.85	4.40	4.95	5.51	6.06	6.61
0.701	3.86	4.59	5.32	6.05	6.79	7.52	8.25
0.784	4.17	5.04	5.92	6.80	7.68	8.56	9.43
0.850	4.60	5.59	6.58	7.58	8.57	9.57	10.56
0.900	4.73	5.98	7.14	8.22	9.20	10.09	10.89
0.944	4.95	6.41	7.67	8.72	9.57	10.21	10.64
0.960	4.96	6.42	7.67	8.70	9.52		
CO_2 –perfluorodecalin ($\text{C}_{10}\text{F}_{18}$)							
0.098	0.73	0.80	0.87	0.95	1.02	1.10	1.17
0.262	1.70	1.91	2.12	2.32	2.53	2.74	2.95
0.349	2.22	2.52	2.83	3.13	3.43	3.73	4.03
0.473	2.90	3.38	3.87	4.35	4.83	5.31	5.79
0.570	3.46	4.11	4.76	5.41	6.06	6.70	7.35
0.674	4.04	4.88	5.73	6.57	7.42	8.26	9.11
0.775	4.50	5.55	6.59	7.64	8.69	9.73	10.78
0.850	4.88	6.07	7.25	8.44	9.62	10.81	12.00
0.900	5.11	6.39	7.68	8.96	10.24	11.53	12.81
0.946	5.32	6.80	8.17	9.43	10.59	11.65	12.60
CO_2 –perfluorobenzene (C_6F_6)							
0.107	0.61	0.72	0.82	0.93	1.04	1.14	1.25
0.199	0.99	1.19	1.38	1.58	1.77	1.97	2.16
0.299	1.49	1.80	2.10	2.40	2.70	3.01	3.31
0.410	2.00	2.45	2.89	3.33	3.77	4.22	4.66
0.510	2.52	3.10	3.68	4.26	4.84	5.42	6.00
0.600	3.00	3.71	4.43	5.15	5.87	6.59	7.30
0.700	3.58	4.48	5.37	6.26	7.15	8.05	8.94
0.800	4.19	5.25	6.32	7.39	8.46	9.53	10.59
0.850	4.49	5.63	6.77	7.91	9.04	10.18	11.32
0.900	4.84	6.17	7.43	8.59	9.68	10.67	11.58
0.950	5.25	6.66	7.90	8.99	9.92	10.68	11.29
CO_2 –perfluorotoluene (C_7F_8)							
0.101	0.63	0.71	0.79	0.87	0.95	1.03	1.12
0.205	1.11	1.30	1.48	1.67	1.86	2.05	2.24
0.302	1.51	1.81	2.10	2.39	2.68	2.98	3.27
0.400	1.99	2.40	2.81	3.22	3.62	4.03	4.44
0.497	2.45	3.00	3.55	4.10	4.65	5.20	5.75
0.603	3.00	3.72	4.43	5.15	5.87	6.59	7.31
0.701	3.62	4.49	5.36	6.23	7.10	7.97	8.84
0.801	4.22	5.27	6.32	7.37	8.42	9.47	10.52
0.872	4.77	5.94	7.12	8.29	9.47	10.64	11.82
0.901	4.95	6.30	7.59	8.80	9.95	11.02	12.02
0.950	5.21	6.72	8.05	9.21	10.18	10.97	11.58
CO_2 –perfluoromethylcyclohexane (C_7F_{14})							
0.099	0.71	0.79	0.88	0.96	1.05	1.14	1.22
0.203	1.27	1.45	1.63	1.81	1.98	2.16	2.34
0.300	1.83	2.09	2.36	2.62	2.88	3.14	3.41
0.401	2.41	2.78	3.14	3.51	3.87	4.24	4.61
0.514	2.99	3.51	4.03	4.55	5.07	5.59	6.11
0.600	3.46	4.10	4.74	5.38	6.02	6.66	7.30
0.701	3.97	4.76	5.55	6.34	7.13	7.92	8.71
0.800	4.46	5.46	6.44	7.39	8.32	9.23	10.10
0.870	4.82	5.91	7.02	8.17	9.22	10.03	10.48
0.900	5.02	6.14	7.34	8.48	9.46	10.13	10.40
0.950	5.40	6.70	7.96	8.99	9.59	9.58	8.77

studied in this work and the corresponding CO_2 /alkane systems. As shown in parts a and b of Figure 5, it was observed that, besides the solubility of carbon dioxide always being higher in the fluorinated systems, the solubility of carbon dioxide in the different structural alkanes is similar, showing the same trends found in the CO_2 /perfluoroalkane mixtures. This observation agrees with the hypothesis stated above that there is no particular interaction between CO_2 and perfluoroalkanes and that the higher solubility of the gas in this system is essentially due to geometric packing and dispersion interactions.

As mentioned previously, the quadrupole term was introduced in the soft-SAFT equation to check its effect on the CO_2 mixtures, as compared to the experimental data. Figures 6, 7, and 8 show a comparison between the experimental data for the systems CO_2 /perfluorobenzene, CO_2 /perfluorotoluene, and CO_2 /perfluoro-*n*-octane, respectively, with predictions from the soft-SAFT equation with and without the quadrupole term, at three different temperatures, 293.15, 323.15, and 353.15 K. Symbols correspond to the experimental data; dashed lines show calculations performed with soft-SAFT without the quadrupole,

F

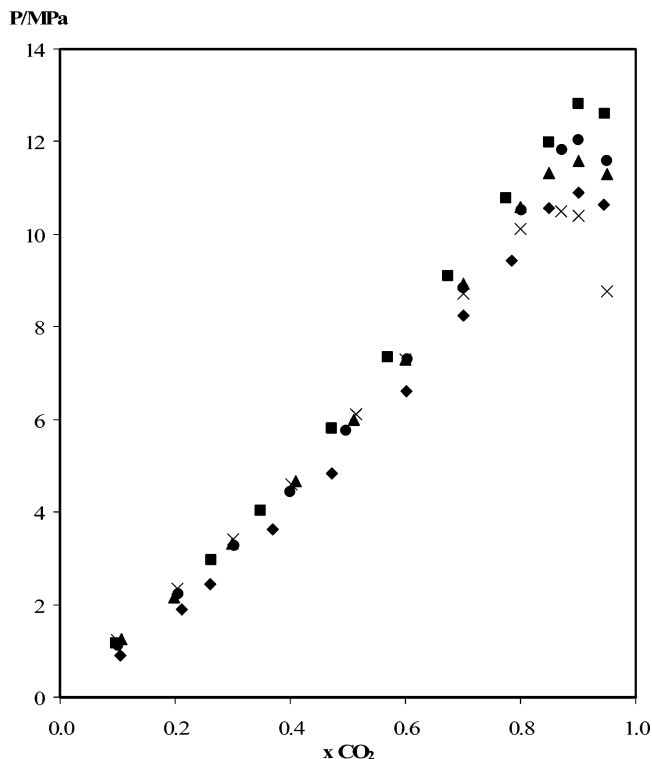


Figure 3. Experimental measured solubility of CO₂ in perfluoroalkanes at 353.15 K: symbols as in Figure 2.

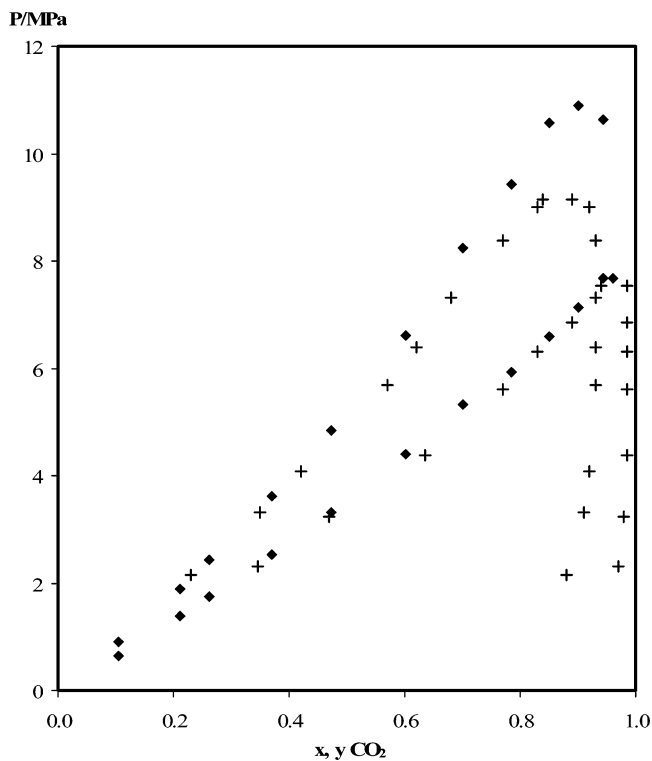


Figure 4. Effect of the chain size on the solubility of CO₂ in perfluoroalkane systems at 313 and 353 K: data measured for CO₂/perfluoro-*n*-octane system in this work (◆) and experimental data measured for CO₂/perfluoro-*n*-hexane system by (+) Iezzi et al.⁵ Note that data presented by Iezzi et al.⁵ for the lower temperature was actually measured at 314.65 K

while the full lines represent calculations with the polar term. It can be observed that the quadrupole has a significant influence on the description of the phase behavior of the mixtures involving aromatic compounds. Polar soft-SAFT is able not only to provide an overall better agreement but also to capture the

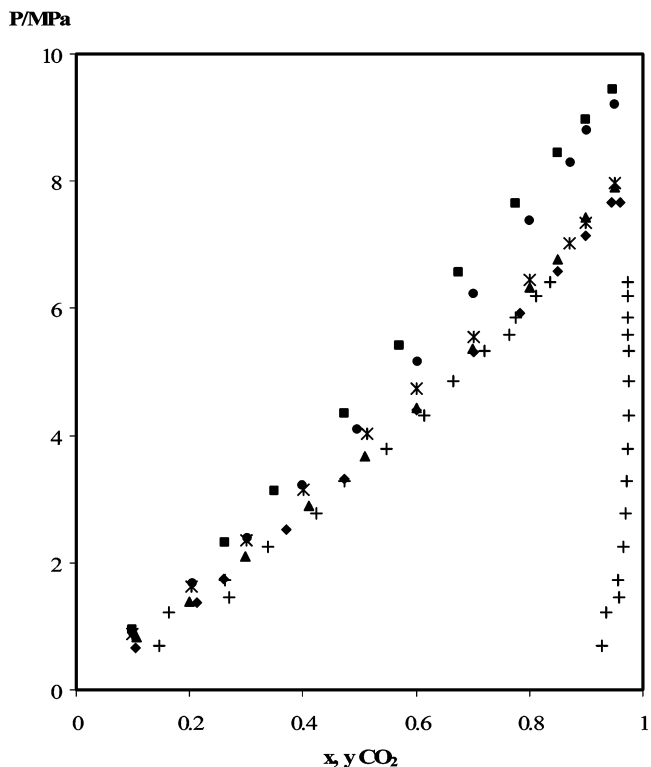
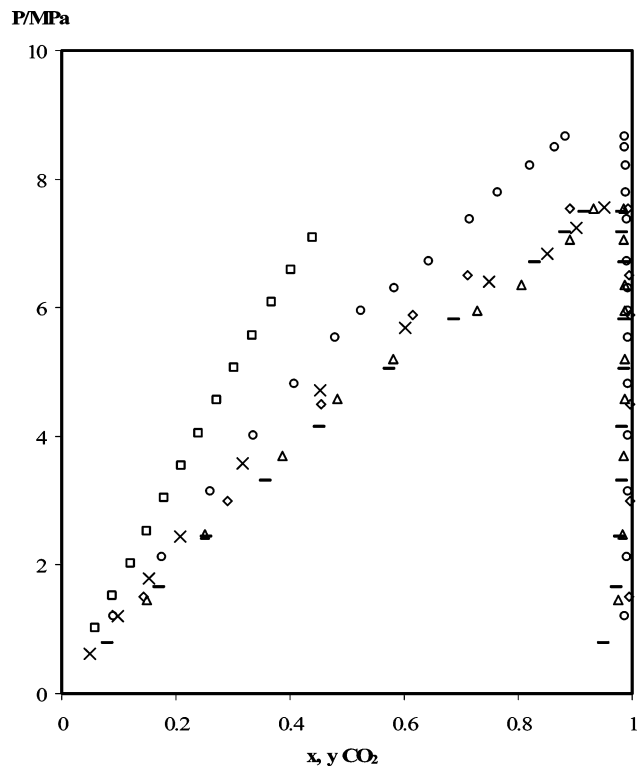


Figure 5. Comparison between the $P-x$ diagrams for (a) the CO₂/alkane mixtures and (b) the corresponding CO₂/perfluoroalkane mixtures at a given temperature of 313 or 323 K depending on the data available on the literature: (—) CO₂/*n*-hexane,³⁹ (◊) CO₂/*n*-octane,⁴⁰ (□) CO₂/decalin,⁴¹ (x) CO₂/methylcyclohexane,⁴² (△) CO₂/benzene,⁴³ and (○) CO₂/toluene.⁶ Data for the CO₂/C₆F₁₄ mixture (+) was taken from the work of Iezzi et al.⁵

changes in the curvature as a function of temperature. Note that no binary parameters were fitted in these cases; the lines are full predictions from the pure-component parameters.

Results obtained for perfluorodecalin and perfluoromethylcyclohexane (not shown here) are similar to the ones obtained

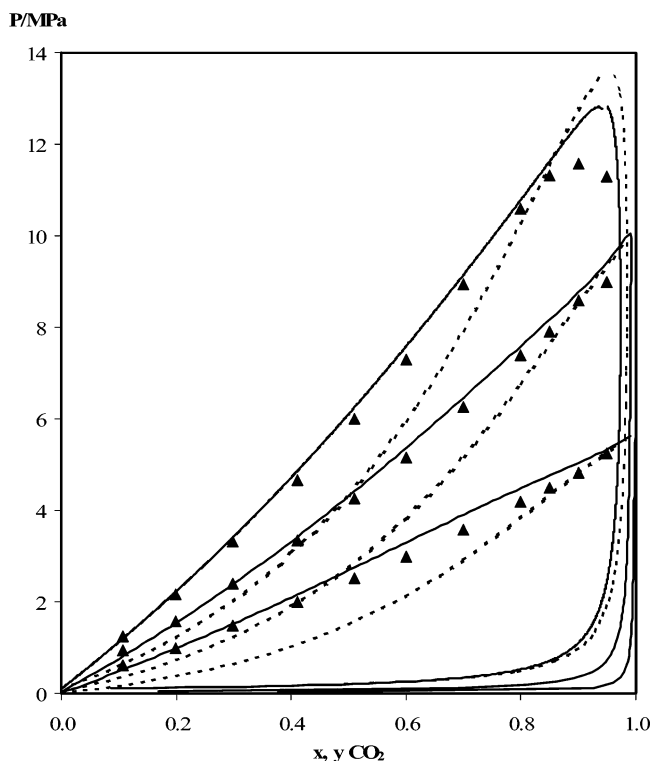


Figure 6. Predictions of the vapor–liquid equilibrium of CO₂/perfluorobenzene system at 293.15, 323.15, and 353.15 K. Symbols represent experimental data measured in this work. Dashed lines correspond to the original soft-SAFT model, and solid lines correspond to the polar soft-SAFT model. In both cases, the size and the energy binary interaction parameters are set to one.

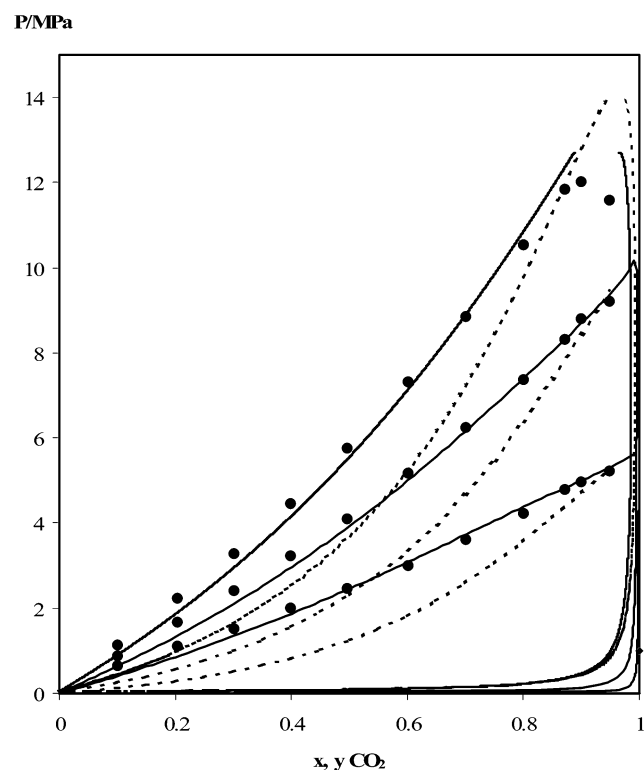


Figure 7. Predictions of the vapor–liquid equilibrium of CO₂/perfluorotoluene system at 293.15, 323.15, and 353.15 K. Legend as in Figure 6.

for perfluoro-*n*-octane, meaning that the introduction of the quadrupole effect does not seem to noticeably influence the description of the phase equilibria for non-aromatic perfluoro-compounds.

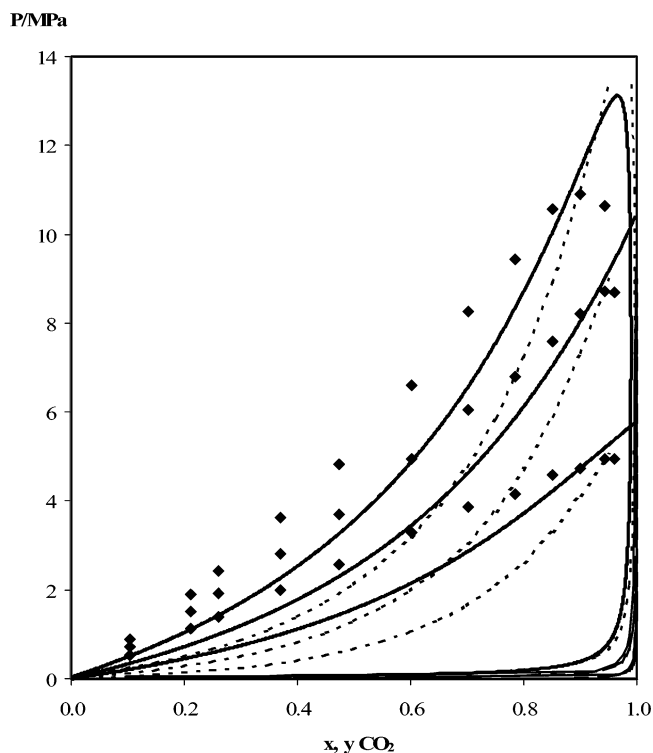


Figure 8. Predictions of the vapor–liquid equilibrium of CO₂/perfluoro-*n*-octane system at 293.15, 323.15, and 323.15 K. Legend as in Figure 6.

Table 3. Optimized Size and Energy Binary Interaction Parameters for the Mixtures Measured in This Work

system	with polar term		without polar term	
	η_{ij}	ξ_{ij}	η_{ij}	ξ_{ij}
CO ₂ –C ₈ F ₁₈	1.04	0.890	1.06	0.790
CO ₂ –C ₁₀ F ₁₈	1.04	0.836	1.06	0.732
CO ₂ –C ₇ F ₁₄	1.04	0.902	1.06	0.806

In previous work, it was observed that binary parameters are needed for obtaining quantitative predictions if the lengths of the two molecules involved in the mixtures are different and/or their shape deviates from spherical.¹⁸ Using another EoS, Kontogeorgis et al.⁴⁴ and Coutinho et al.⁴⁵ showed that, for athermal mixtures, the use of a size binary parameter would provide a better and more meaningful description of the data and that the use of this parameter would reduce the size of the energy binary parameter to be used in systems where energetic interactions are important. As previously with oxygen/perfluorocarbons,¹⁹ a good description of the phase diagrams of CO₂/perfluoroalkanes requires the use of two interaction parameters. One of the main advantages of using a molecular-based EoS is that parameters should not depend on the thermodynamic conditions. In our case, the P – x curves were found to be sensitive to the energy binary parameter, ξ_{ij} , but relatively insensitive to the binary size parameter, η_{ij} . Hence, the procedure followed here was to fix the binary size parameter and adjust only the energy parameter to experimental data at 323.15 K for each mixture. In this way, the size and energy binary parameters were transferred within the same mixture at different conditions. Additionally, the size parameter was also transferred for different compounds.

Table 3 compares the binary parameters adjusted when the quadrupole moment is considered explicitly and in an effective way. When the polar term is included, the binary energy and size parameters are consistently closer to unity than when the nonpolar soft-SAFT EoS is used. This is expected, since the polar equation explicitly considers the quadrupole, with an extra

P/MPa

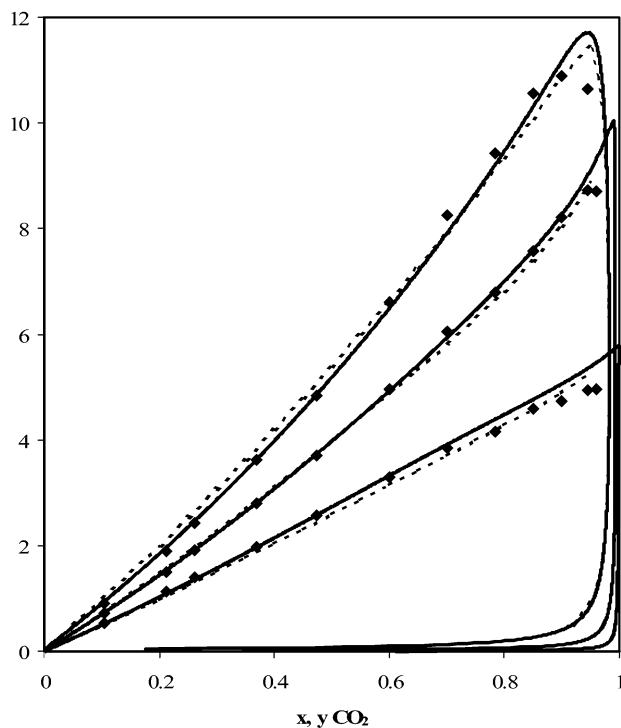


Figure 9. Vapor–liquid equilibrium of CO₂/perfluoro-*n*-octane system at 293.15, 323.15, and 353.15 K. Symbols represent experimental data measured in this work. Solid lines correspond to the soft-SAFT model including the polar term, and black dashed lines correspond to the original soft-SAFT model at optimized size and energy binary interaction parameters (Table 3).

P/MPa

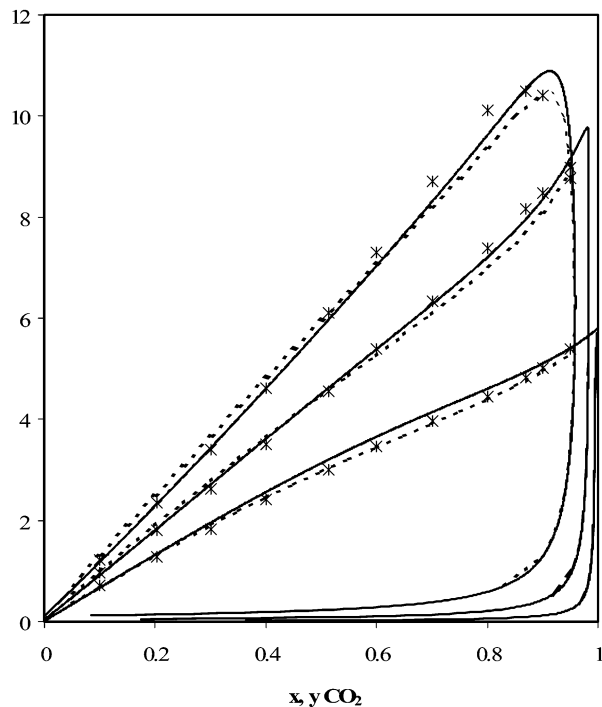


Figure 10. Vapor–liquid equilibrium of CO₂/perfluoromethylcyclohexane system at 293.15, 323.15, and 353.15 K. Legend as in Figure 9.

parameter; in this case, the binary parameters account only for the unlike van der Waals interactions. On the contrary, when the quadrupole is not included, the binary parameters, especially the energy parameter, effectively account for it, showing greater deviations from unity.

P/MPa

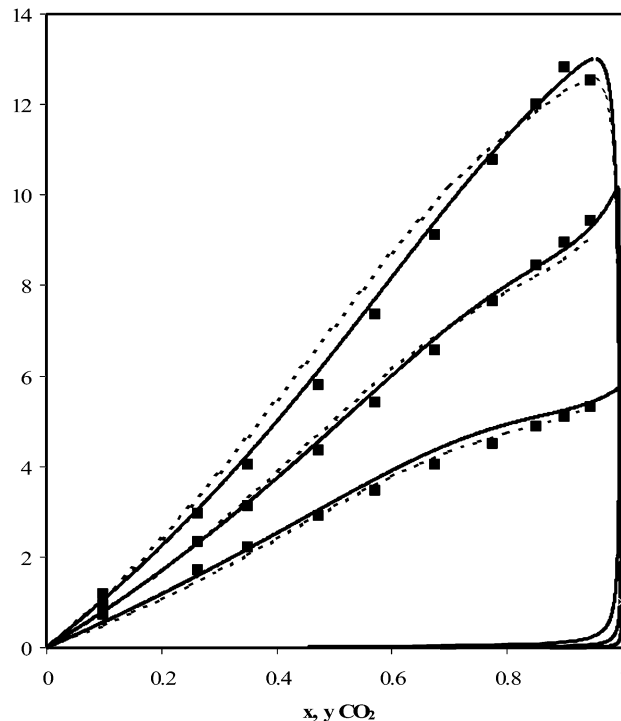


Figure 11. Vapor–liquid equilibrium of CO₂/perfluorodecalin system at 293.15, 323.15, and 353.15 K. Legend as in Figure 9.

Figures 9, 10, and 11 present P – x diagrams where experimental data for the binary mixtures CO₂/perfluoro-*n*-octane, CO₂/perfluoromethylcyclohexane, and CO₂/perfluorodecalin, respectively, are compared against the soft-SAFT calculations. The energy binary parameter was adjusted for each mixture to the intermediate temperature (323.15 K) and used in a predictive manner for the other temperatures. The binary size parameter used for the three mixtures was constant, equal to 1.04 for the polar soft-SAFT EoS and to 1.06 for the original soft-SAFT EoS. It can be observed that agreement between the experimental data and the description provided by the soft-SAFT model with and without the polar term are both excellent for the three mixtures, at all conditions studied.

Conclusions

New high-pressure equilibrium phase diagrams for CO₂/perfluoroalkane mixtures at temperatures ranging from 293.15 to 353.15 K have been measured. The different chemical natures of the perfluoroalkanes were chosen to investigate its possible influence on the solubility behavior. It has been observed that the solubility of CO₂ in the selected perfluoroalkanes is very similar, with a temperature dependence more pronounced in the case of the aromatic compounds, meaning that enthalpic interactions are more important on these systems.

The experimental data has been modeled with both the original and a modified version of the soft-SAFT EoS that takes into account the quadrupolar interactions. For the CO₂/perfluoroaromatic mixtures studied, polar soft-SAFT with pure-component molecular parameters was able to provide quantitative predictions of the experimental data, for the entire temperature range studied. To quantitatively describe the other mixtures, a size binary interaction parameter was fixed for all the mixtures and the energy binary interaction parameter was adjusted. The results here reported seem to indicate that the

quadrupole is only important for the description of systems of CO₂ with perfluoroaromatic compounds.

Acknowledgment

A.M.A.D. is grateful to Fundação para a Ciência e Tecnologia (Ph.D. Grant SFRH/BD/5390/2001). We also acknowledge financial support from the Portuguese government through Project POCTI/43356/2001 and from the Spanish government under Projects PPQ2001-0671, HP2002-0089, and CTQ2004-05985-02-01.

List of Symbols

A = Helmholtz energy
 g = radial distribution function
 m = chain length, number of Lennard-Jones segments
 Q = quadrupole moment (C·m²)
 R = real gas constant
 T = temperature
 x = molar fraction

Greek Symbols

ϵ = soft-SAFT Lennard-Jones energy parameter
 η = soft-SAFT binary interaction parameter for size
 ξ = soft-SAFT binary interaction parameter for energy
 σ = soft-SAFT Lennard-Jones size parameter (segments diameter)

Superscripts

assoc = related to association contributions
 chain = related to chain-bonding contributions
 ideal = related with the ideal-gas contribution
 polar = related to polar-moments contributions
 ref = reference-term contributions
 total = total sum of the contributions

Subscripts

i = component i
 j = component j
 LJ = Lennard-Jones

Literature Cited

- Wasanasathian, A. A.; Peng, C.-A. Enhancement of microalgal growth by using perfluorocarbon as oxygen carrier. *Artif. Cells, Blood Substitutes, Immobilization Biotechnol.* **2001**, *29*, 47.
- Raveendran, P.; Wallen, S. L. Cooperative C—H···O Hydrogen Bonding in CO₂–Lewis Base Complexes: Implications for Solvation in Supercritical CO₂. *J. Am. Chem. Soc.* **2002**, *124*, 12590.
- Stone, M. T.; Rocha, S. R. P.; Rossky, P. J.; Johnston, K. P. J. Molecular Differences between Hydrocarbon and Fluorocarbon Surfactants at the CO₂/Water Interface. *J. Phys. Chem. B* **2003**, *107*, 10185.
- Hoeffling, T. A.; Enick, R. M.; Beckman, E. Microemulsions in Near-Critical and Supercritical Carbon Dioxide. *J. Phys. Chem.* **1991**, *95*, 7127.
- Iezzi, A.; Bendale, P.; Enick, R.; Turberg, M.; Brady, J. ‘Gel’ Formation in Carbon Dioxide–Semifluorinated Alkane Mixtures and Phase Equilibria of a Carbon Dioxide–Perfluorinated Alkane Mixture. *Fluid Phase Equilib.* **1989**, *52*, 307.
- Lazzaroni, M. J.; Bush, D.; Brown, J. S.; Eckert, C. A. High-pressure vapor–liquid equilibria of some carbon dioxide plus organic binary systems. *J. Chem. Eng. Data* **2005**, *50*, 60.
- Cece, A.; Jureller, S. H.; Kerschner, J. L. Molecular Modeling Approach for Contrasting the Interaction of Ethane and Hexafluoroethane with Carbon Dioxide. *J. Phys. Chem.* **1996**, *100*, 7435.
- Dardin, A.; DeSimone, J. M.; Samulski, E. T. Fluorocarbons Dissolved in Supercritical Carbon Dioxide. NMR Evidence for Specific Solute–Solvent Interactions. *J. Phys. Chem. B* **1998**, *102*, 1775.
- Diep, P.; Jordan, K. J.; Johnson, J. K.; Beckman, E. J. CO₂–Fluorocarbon and CO₂–Hydrocarbon Interactions from First-Principles Calculations. *J. Phys. Chem. A* **1998**, *102*, 2231.

- Yee, G. G.; Fulton, J. L.; Smith, R. D. Fourier Transform Infrared Spectroscopy of Molecular Interactions of Heptafluoro-1-butanol or 1-butanol in Supercritical Carbon Dioxide and Supercritical Ethane. *J. Phys. Chem.* **1992**, *96*, 6172.

- Yonker, C. R.; Palmer, B. J. Investigation of CO₂/Fluorine Interactions through the Intermolecular Effects on the ¹H and ¹⁹F Shielding of CH₃F and CHF₃ at Various Temperatures and Pressures. *J. Phys. Chem. A* **2001**, *105*, 308.

- Cui, S. T.; Cochran, H. D.; Cummings, P. T. Vapor–Liquid-Phase Coexistence of Alkane–Carbon Dioxide and Perfluoroalkane–Carbon Dioxide Mixtures. *J. Phys. Chem. B* **1999**, *103*, 4485.

- Gomes, M. F. C.; Padua, A. H. Interactions of Carbon Dioxide with Liquid Fluorocarbons. *J. Phys. Chem. B* **2003**, *107*, 14020.

- Zhang, L.; Siepmann, J. I. Pressure Dependence of the Vapor–Liquid–Liquid-Phase Behavior in Ternary Mixtures Consisting of n -Alkanes, n -Perfluoroalkanes, and Carbon Dioxide. *J. Phys. Chem. B* **2005**, *109*, 2911.

- Colina, C. M.; Galindo, A.; Blas, F. J.; Gubbins, K. E. Phase Behavior of Carbon Dioxide Mixtures With n -alkanes and n -perfluoroalkanes. *Fluid Phase Equilib.* **2004**, *222*, 77.

- Gil-Villegas, A.; Galindo, A.; Whitehead, P. J.; Mills, S. J.; Jackson, G.; Burgess, A. N. Statistical Associating Fluid Theory for Chain Molecules with Attractive Potentials of Variable Range. *J. Chem. Phys.* **1997**, *106*, 4168.

- Blas, F. J.; Vega, L. F. Thermodynamic Behaviour of Homonuclear and Heteronuclear Lennard-Jones Chains With Association Sites from Simulation and Theory. *Molecular Physics* **1997**, *92*, 135.

- Blas, F. J.; Vega, L. F. Prediction of Binary and Ternary Diagrams Using the Statistical Associating Fluid Theory (SAFT) Equation of State. *Ind. Eng. Chem. Res.* **1998**, *37*, 660.

- Dias, A. M. A.; Bonifácio, R. P.; Marrucho, I. M.; Pádua, A. A. H.; Gomes, M. F. C. Solubility of Oxygen in n -hexane and in n -perfluorohexane. Experimental Determination and Prediction by Molecular Simulation. *Phys. Chem. Chem. Phys.* **2003**, *5*, 543.

- Pàmies, J. C. Ph.D. Dissertation, Universitat Rovira i Virgili, Tarragona, Spain, 2003.

- Pauly, J.; Daridon, J. L.; Coutinho, J. A. P. *Fluid Phase Equilib.* **2005**, submitted for publication.

- Chapman, W. G.; Gubbins, K. E.; Jackson, G.; Radosz, M.; New Reference Equation of State for Associating Liquids. *Ind. Eng. Chem. Res.* **1990**, *29*, 1709.

- Huang, S. H.; Radosz, M. Equation of State for Small, Large, Polydisperse, and Associating Molecules. *Ind. Eng. Chem. Res.* **1990**, *29*, 2284.

- Gross, J.; Sadowski, G. Perturbed-Chain SAFT: An Equation of State Based on a Perturbation Theory for Chain Molecules. *Ind. Eng. Chem. Res.* **2001**, *40*, 1244.

- Muller, E. A.; Gubbins, K. E. Molecular-Based Equations of State for Associating Fluids: A Review of SAFT and Related Approaches. *Ind. Eng. Chem. Res.* **2001**, *40*, 2193.

- Economou, I. G. Statistical Associating Fluid Theory: A Successful Model for the Calculation of Thermodynamic and Phase Equilibrium Properties of Complex Fluid Mixtures. *Ind. Eng. Chem. Res.* **2002**, *41*, 953.

- Johnson, J. K.; Zollweg, J. A.; Gubbins, K. E. The Lennard-Jones Equation of State Revisited. *Mol. Phys.* **1993**, *78*, 591.

- Gubbins, K. E.; Two, C. H. Thermodynamics of Polyatomic Fluid Mixtures—I. Theory. *Chem. Eng. Sci.* **1978**, *33*, 863.

- Stell, G.; Rasaiah, J. C.; Narang, H. Thermodynamic Perturbation-Theory for Simple Polar Fluids. *Mol. Phys.* **1974**, *27*, 1393.

- Two, C. H.; Gubbins, K. E.; Gray, C. G. Excess Thermodynamic Properties for Liquid-Mixtures of Non-Spherical Molecules. *Mol. Phys.* **1975**, *29*, 713.

- Two, C. H. Ph.D. Dissertation, University of Florida, Gainesville, FL, 1976.

- Jog, P. K.; Chapman, W. G. Application of Wertheim’s Thermodynamic Perturbation Theory to Dipolar Hard Sphere Chains. *Mol. Phys.* **1999**, *97*, 307.

- Vrabec, J.; Stoll, J.; Hasse, H. A Set of Molecular Models for Symmetric Quadrupolar Fluids. *J. Phys. Chem. B* **2001**, *105*, 12126.

- Vrbancich, J.; Ritchie, G. L. D. Quadrupole Moments of Benzene, Hexafluorobenzene and other Nondipolar Aromatic Molecules. *J. Chem. Soc., Faraday Trans. 2* **1980**, *76*, 648.

- Casas, S. P.; Trujillo, J. H.; Costas, M. Experimental and Theoretical Study of Aromatic–Aromatic Interactions. Association Enthalpies and Central and Distributed Multipole Electric Moments Analysis. *J. Phys. Chem. B* **2003**, *107*, 4167.

- NIST Chemistry WebBook; NIST Standard Reference Database Number 69; Linstrom, P. J., Mallard, W. G., Eds.; National Institute of

Standards and Technology: Gaithersburg, MD, 2003; p 20899 (<http://webbook.nist.gov>).

(37) Dias, A. M. A.; Gonçalves, C. M. B.; Caço, A. I.; Santos, L. M. N. B. F.; Piñeiro, M. M.; Vega, L. F.; Coutinho, J. A. P.; Marrucho, I. M. Densities and vapor pressures of highly fluorinated compounds. *J. Chem. Eng. Data* **2005**, *50*, 1328.

(38) Glew, D. N.; Reeves, L. W. Purification of Perfluoro-heptane and Perfluoromethylcyclohexane. *J. Phys. Chem.* **1956**, *60*, 615.

(39) Ohgaki, K.; Katayama, T. Isothermal Vapor–Liquid Equilibrium Data for Binary Systems Containing Carbon Dioxide at High Pressures: Methanol–Carbon Dioxide, *n*-Hexane–Carbon Dioxide, and Benzene–Carbon Dioxide Systems. *J. Chem. Eng. Data* **1976**, *21*, 54.

(40) Li, Y. H.; Dillard, K. H.; Robinson, R. L. Vapor–Liquid-Phase Equilibrium for Carbon Dioxide–*n*-Hexane at 40, 80 and 120 °C. *J. Chem. Eng. Data* **1981**, *26*, 53.

(41) Weng, W. L.; Lee, M. J. Vapor–Liquid Equilibrium of the Octane/Carbon Dioxide, Octane/Ethane, and Octane/Ethylene Systems. *J. Chem. Eng. Data* **1992**, *37*, 213.

(42) Tiffin, D. L.; DeVera, A. L.; Luks, K. D.; Kohn, J. P. Phase-Equilibria Behavior of the Binary Systems Carbon Dioxiden Butylbenzene and Carbon Dioxide–*trans*-Decalin. *J. Chem. Eng. Data* **1978**, *23*, 45.

(43) Nasrifar, Kh; Heuvel, M. M. M.; Peters, C. J.; Ayatollahi, Sh.; Moshfeghian, M. Measurements and Modeling of Bubble Points in Binary Carbon Dioxide Systems with Tetrahydropyran and Methylcyclohexane. *Fluid Phase Equilib.* **2003**, *204*, 1.

(44) Kontogeorgis, G. M.; Coutsikos, P.; Harismiadis, V. L.; Fredenslund, A.; Tassios, D. P. A Novel Method for Investigating the Repulsive and Attractive Parts of Cubic Equations of State and the Combining Rules Used With the vdW-1f Theory. *Chem. Eng. Sci.* **1998**, *53*, 541.

(45) Coutinho, J. A. P.; Kontogeorgis, G. M.; Stenby, E. H. Binary interaction parameters for nonpolar systems with cubic equations of state: A theoretical approach. 1. CO₂/hydrocarbons using SRK equation of state. *Fluid Phase Equilib.* **1994**, *102*, 31.

Received for review September 10, 2005

Revised manuscript received December 12, 2005

Accepted January 24, 2006

IE051017Z